

NOTICE CONCERNING COPYRIGHT RESTRICTIONS

This document may contain copyrighted materials. These materials have been made available for use in research, teaching, and private study, but may not be used for any commercial purpose. Users may not otherwise copy, reproduce, retransmit, distribute, publish, commercially exploit or otherwise transfer any material.

The copyright law of the United States (Title 17, United States Code) governs the making of photocopies or other reproductions of copyrighted material.

Under certain conditions specified in the law, libraries and archives are authorized to furnish a photocopy or other reproduction. One of these specific conditions is that the photocopy or reproduction is not to be "used for any purpose other than private study, scholarship, or research." If a user makes a request for, or later uses, a photocopy or reproduction for purposes in excess of "fair use," that user may be liable for copyright infringement.

This institution reserves the right to refuse to accept a copying order if, in its judgment, fulfillment of the order would involve violation of copyright law.

Geothermal Exploration Using Gravity Gradiometry – a Salton Sea Example

S. Bruce Kohn¹, Chloe Bonet², Dan DiFrancesco¹, Helen Gibson²

¹Lockheed Martin, Niagara Falls NY

²Intrepid Geophysics, Perth, Australia

Keywords

Geothermal, geophysics, gravity gradiometry, exploration, Salton Sea, EGS

ABSTRACT

Gravity methods are sensitive to the subsurface distribution of geologic materials of different densities, and have proven value in geothermal exploration. In some geothermal settings, measurements of the earth's gravity gradient (i.e., gravity gradiometry) may provide advantages over the more traditional measurements of the earth's scalar gravity field. These include higher resolution of targets less than approximately 10 km deep, and better edge detection for interpreting faults, boundaries of geologic bodies, and other structural features.

To determine if the gravity gradient signal from a geothermal exploration target is within the detection limits of commercially available sensor technology, the gravity gradient response was modeled for a simplified 3D geological model of the Salton Sea Geothermal Field in Southern California. This is a water-dominated geothermal field in the Salton Trough with a known 20 mGal residual gravity anomaly.

The resulting gradient of vertical gravity in the z direction (G_{zz}) at the Salton Sea Geothermal Field ranged from -53 to -31 Eötvös (1 Eötvös = $0.1\mu\text{Gal}/\text{m}$, which is equivalent to 0.1 ppb of the Earth's gravity field). The local density highs are clearly visible in the calculated gravity gradient response, and are consistent with the known gravity anomaly. Additionally, modeled hypothetical faults associated with the pull apart basin setting are more clearly evident in the gravity gradient data compared with the scalar gravity data. This has significance for exploration of blind geothermal systems, especially where faults do not have surface expression in the cover geology.

1. Introduction

Gravity methods have proven value in geothermal exploration, and ground-based scalar gravity surveys are a standard reconnais-

sance tool for geothermal explorationists.¹ Since the mid-1990s, airborne gravity gradiometry has been a cost-effective addition to the tool belt of hydrocarbon and mineral explorationists. The objective of this paper is to examine the potential of the application of gravity gradiometry to geothermal exploration.

In Section 2 below, we provide a brief overview of the traditional measurement of the earth's gravity field (i.e., scalar gravity), as well as gravity gradiometry – a more innovative method. Section 3 briefly describes the application of gravity methods for geothermal exploration. In Section 4, the potential application of gravity gradiometry for geothermal exploration is examined by forward modeling the gravity response of a geological scenario based on the Salton Sea Geothermal Field, which is associated with a known gravity anomaly. Finally, the results of the modeling exercise are discussed and summarized in the conclusions.

2. The Gravity and Gravity Gradiometry Methods

A gravimeter measures the magnitude of the vertical component of the Earth's gravity field, a scalar quantity. A gravity gradiometer measures the gradient – the spatial rate of change

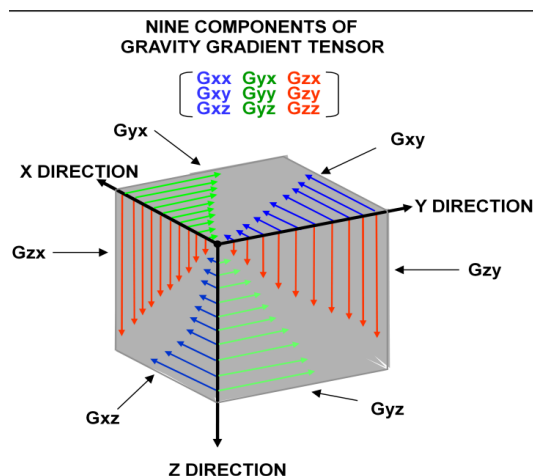


Figure 1. Spatial variations in three orthogonal directions of the components of the gravity field.

– of the earth’s gravity field, which is a vector quantity with both magnitude and direction. For each component direction (x, y and z) of the gravity field, there are three components of change (e.g., the rate of change of the z component of gravity in the x direction, or G_{zx}). There are nine possible quantities to be measured, which can be arranged in a 3 x 3 matrix called the gravity gradient tensor (Fig. 1). Five of these are independent.

Mobile gravity gradiometry, developed for the US Navy in the 1970s and commercialized in the 1990s, has certain advantages over scalar gravity for exploration. First, gradiometry has higher near-field resolution than scalar gravity for geophysical targets less than approximately 10 km deep, because gradient measurements resolve smaller wavelengths than gravity methods. However, the gradient signal decreases with the cube of the distance from the target, whereas the scalar gravity signal decreases with the square of the distance, which means that gradiometry can be more effective than scalar gravity for shallow (or close) sources and features. This has proven application for mineral exploration settings with relatively near-surface targets and for the delineation of sedimentary basins for hydrocarbon exploration.

Second, gradiometry provides better edge detection. Scalar gravity identifies the center of mass of a target, whereas the gravity gradient changes most rapidly at the edges of geophysical targets, and can be used to delineate the extent of mineral deposits, faults, and other structural features.

Third, gravity gradiometry involves multiple, independent data sets that provide additional constraints for data inversion, addressing some of the ambiguity inherent in potential fields methods.

Finally, airborne gravity gradiometry surveys can be cost effective and quicker than surface scalar gravity for regional surveys, and are not impacted by limitations on the ground due to cultural sensitivities, vegetation, surface water and inaccessible terrain. Standard data corrections for ocean tides, lunar motion, barometric pressure, etc., are not required when processing gravity gradient data.

3. Applications in Geothermal Exploration

Gravity methods are sensitive to the subsurface distribution of geologic materials of different densities. Ground-based scalar gravity surveys have proven value in the exploration of conventional hydrothermal systems by identifying subsurface anomalies associated with deep magmatic bodies, granitic bodies, zones of hydrothermal alteration and fault structures. For example, zones of alteration that may be indicative of geothermal activity typically have a density contrast with the surrounding unaltered rock, and may thus have measurable scalar gravity and gravity gradient signals. This is the case in the Salton Sea Geothermal Field, as described below.

Also, geothermal activity is usually associated with fault structures that provide preferential pathways through the subsurface for the circulation of geothermal fluids. Often, these fault structures do not manifest themselves at the surface because they are concealed by younger sedimentary cap-rock sequences, and thus the faults are difficult to detect and map. As is shown below, gravity gradiometry may be useful for the detection of blind geothermal systems such as these.

While conventional hydrothermal systems for geothermal energy are controlled by fault systems (and faults are a desirable component of these systems), the opposite is sometimes true for engineered geothermal systems (EGS). In EGS, undetected and undesirable faults may result in the loss of injected geothermal fluids. However, faults may also positively contribute to sustainable circulation through an engineered system. In either case, full knowledge of fault character and location is imperative in EGS plays.

4. Salton Sea Geothermal Field: Modelling 3D Geology and Gravity Gradiometry

Introduction

A new 3D geology model of the Salton Sea Geothermal Field was constructed for the purpose of carrying out forward gravity and gravity gradiometry modelling. The model was built using 3D GeoModeller software and is a simplified representation of part of the Salton Sea Trough (Table 1). Some constraining geologic data for the model were acquired from the published literature. Additionally, some geological features of the model are fictional (including the sub-vertical faults), devised to represent features which are known to occur, but for which no constraining data for their location was publicly available.

Table 1. Dimensions of the project cube of the 3D geology model of the Salton Sea Trough, built for forward gravity and gradiometry modelling. Projection system and datum: WGS 84 / UTM zone 11N.

	Minimum	Maximum	Range
East	617 101 E	662 885 E	45, 784 m
North	3 624 260 N	3 688 680 N	64,420 m
Z (+ve is up)	-7,000 m	+2,000 m	9,000 m

Geological Setting

The Salton Sea Geothermal Field (GF) is located in the Salton Trough, southern California. The setting is characterized by local zones of extension along a divergent plate boundary. High-angle basin bounding faults contribute to the rift-basin architecture and accommodate subsidence which has resulted in the accumulation of Pleistocene and Holocene aged sequences (Brothers et al., 2009). Sediments within the Salton Trough are relatively undeformed. Crustal thinning is a feature of this region and causes anomalous levels of heat from mantle-derived magmas to affect the sedimentary sequences (Younker et al., 1981).

Known Gravity Anomaly

In the Salton Sea GF, heat is generally transferred by the lateral spreading of hot water beneath impermeable cap rock layers, resulting in hydrothermal alteration (Younker et al., 1981). A known +20 mGal residual gravity anomaly exists in the Salton Sea GF, and is interpreted to be associated with zones of higher density due to hydrothermal alteration of reservoir rocks, and to high temperatures (Kasameyer and Hearst, 1988).

3D Geology Modeling

For the purposes of building a simplified 3D geological model we adopted the general rock-type categories identified

by Younker et al., 1981. Generally proceeding from shallowest to deepest they are: i) low-permeability cap rock, ii) upper reservoir rocks consisting of sandstones, siltstones, and shales

Formation	Density (g/cm ³)
Cover	Normal(1.8,0,100)
Cap_rock	Normal(2.1,0,100)
A_0	Normal(2.15,0,100)
A_1	Normal(2.5,0,100)
B_1	Normal(2.2,0,100)
B_2	Normal(2.6,0,100)
C_1	Normal(2.45,0,100)
C_2	Normal(2.65,0,100)
Basement	Normal(2.67,0,100)

Figure 2. Left: Stratigraphic pile for the simplified Salton Sea Geothermal Field geological model; Right: Mean densities assigned to each lithology in the geological model (first variable in brackets).



Figure 3. SW to NE cross-section view of the Salton Sea GF geological model, showing zones of high alteration (units A_1, B_2 and C_2; refer to Fig. 1) which mimic the shape of the underlying basement high.

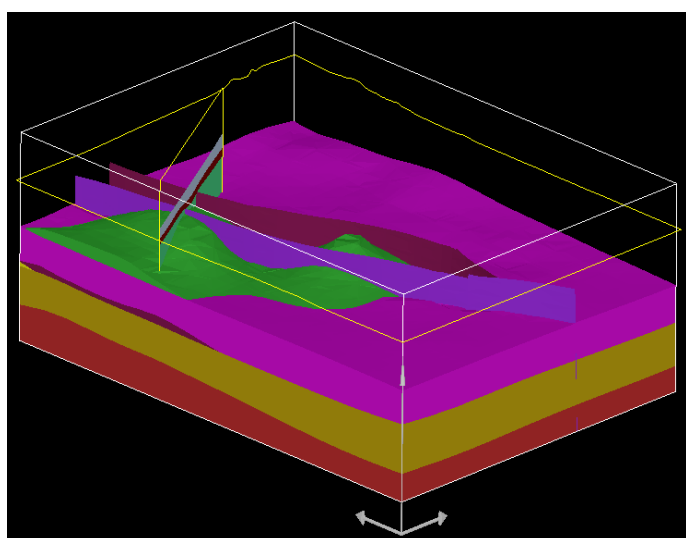


Figure 4. Oblique view from the SW corner of the 3D model of the Salton Sea GF. The vertical exaggeration: (3:1) highlights the dome-like nature of the alteration zones (e.g., A-1 in green), which in-turn reflects the dome-like nature of the underlying basement lithology (red). The rendered 2D section from Fig. 3 is also shown in this 3D view.

that are subject to minor alterations, and iii) lower reservoir rocks that are extensively altered. Compared with our simplified stratigraphic column (Fig. 2) these relate to i) cap-rock; ii) units A_0, B_1 and C_1 (upper reservoir), and iii) units A_1, B_2 and C_2 (lower reservoir).

Notable features of the 3D geology model are the zones of high alteration (units A_1, B_2 and C_2) which mimic the shape of underlying basement highs (Figs. 3 and 4). Note too the high-angle, basin-bounding faults do not interact with the younger cap rock and cover units (Fig. 3).

Forward Gravity and Gravity Gradiometry Modeling

For the purposes of forward gravity modeling, a voxelised grid of the 3D geology model was created at a constant cell size of: $x=300\text{m}$; $y=400\text{m}$ and $z=25\text{m}$. A voxel of variable densities was created based on the variability of lithologies in the voxel model (See Fig. 2, right-side). Mean density values per geological unit were source from the published literature, or estimated. Higher densities were assigned to each of the three lower reservoir units (A_1, B_2, and C_2) compared with the densities of their paired upper reservoirs (A_0, B_1, and C_1). See Fig. 2.

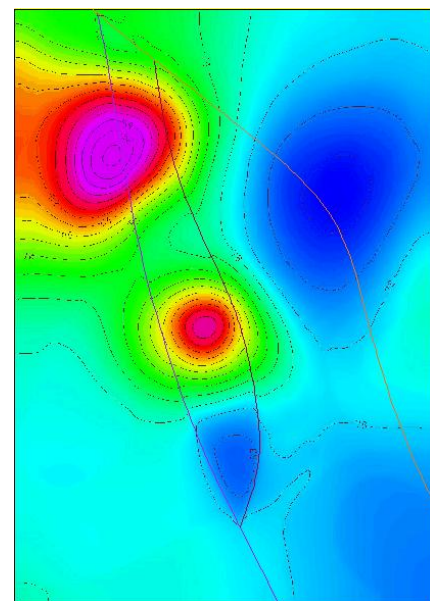
Results

The simulated responses of the free air gravity (G_z) and gradient of vertical gravity in the z direction (G_{zz} , one of the five independent tensors of the gravity field) were computed for the Salton Sea GF. Both were calculated at depth, on a sub-surface horizontal plane above the target alteration zones to eliminate the effects of terrain. The plane of observation was at -300m , which is 600m above the top of highly altered formation A1, 2200m above the top of highly altered B2, and 3250m above the top of highly altered C2. The resulting scalar gravity response ranged from -49 to -82 mGal (Fig. 5). The resulting G_{zz} ranged from -53 to -31 Eötvös (Fig. 6).

The local density highs are clearly visible in the calculated scalar gravity and

Figure 5. Forward modelled gravimetry (free air) overlain by a projected trace of the modelled faults in the Salton Sea GF model.

Range: -49 to -82 mGal. The locations of the dome-like hydro-thermal alteration zones in units A_1, B_2 and C_2, and the locations of basement highs (see Fig. 3) are clearly discernable as gravity anomalies.



gravity gradient responses, and they are consistent with the known gravity anomaly (Figs. 5 and 6). The anomalies are spatially correlated with the high density alteration zones that are in turn centered over the basement highs in the project zone.

The high-angle, basin-bounding faults are only clearly evident in the gravity gradient response (Fig. 6), and virtual absent in the scalar gravity data (Fig. 5). This is significant for exploration of blind geothermal systems, where faults don't have surface expression in the cover geology.

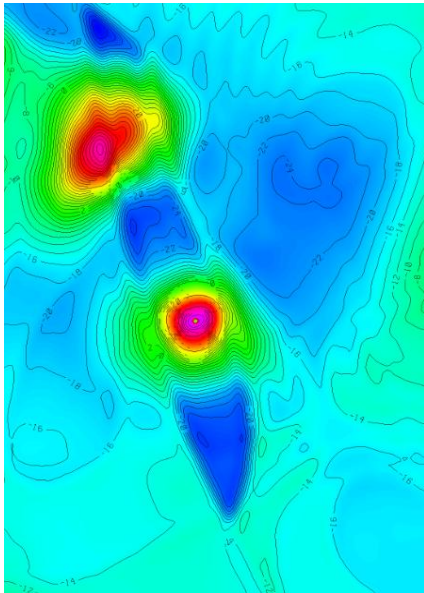


Figure 6. Forward modelled Gzz signal computed for an observation height of -300m. Range: +53 to -14 Eötvös. Note the Gzz shows more detailed resolution of the density anomalies, and (unlike the scalar gravity field) gives a clear sense of off-set associated with the bounding faults (fault traces represented only in Fig. 5).

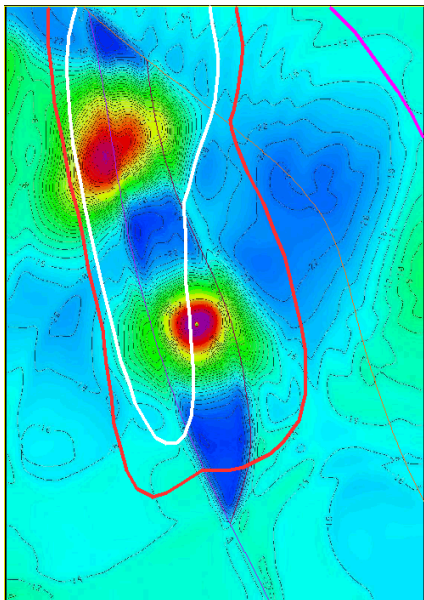


Figure 7. Forward modelled Gzz signal computed for an observation height of -300m (range: +53 to -14 Eötvös), overlain by a plan view of the modelled high-angle faults, in addition to outlines of: i) the outer limit of high surface heat flow (>100 W/m²) –cyan line; ii) the outer limit of the hypersaline brine reservoir –red line; and iii) the outer limit of high formation temperatures (≥ 240°C at ≤ 3km depth) –white line. Delineations reproduced after work by Lachenbruch et al., 1985.

The local density highs modelled in this study are also spatially consistent with the known limits of local zones of: i) high surface heat flow (cyan line); ii) the hypersaline brine reservoir (red line), and iii) high formation temperatures (white

line) – as defined in work by Lachenbruch et al., 1985 and reproduced in Figure 7.

5. Future Work

Rather than ignoring the effects of terrain, future work on this project will correct the gravity gradient for variations in terrain (by upward continuation) to determine if the values fall within the expected range of commercially available instrumentation deployed for surface and airborne surveys.

6. Conclusions

The results of the Salton Sea GF geological and gravity modeling reveal that:

- Local density highs associated with zones of hydrothermal alteration and high temperatures, are clearly visible in the calculated scalar gravity and gravity gradient responses.
- Only the gravity gradient response (Gzz) provides a high resolution signal, and enables clear delineation of the off-set zones associated with high-angle, basin-bounding faults in the Salton Sea GF.

Gravity gradiometry has advantages over scalar gravity methods for geothermal resource exploration, including:

- Higher resolution of targets less than approximately 10 km deep,
- Better edge detection for interpreting faults, boundaries of geologic bodies, and other structural features manifesting density contrasts
- Airborne gravity gradiometry surveys can be cost effective and quicker than surface scalar gravity surveys for regional surveys, and are not impacted by the usual limitations of cultural features at the ground level.

References

- Brothers, D., N. Driscoll, G. Kent, J. Harding, J. Babcock, and R. Baskin, 2009. "Tectonic evolution of the Salton Sea inferred from seismic reflection data." *Nature Geoscience Letters*, Published Online, 26 July 2009.
- Kasameyer, P. W., and J. R. Hearst, 1988. "Borehole Gravity Measurements in the Salton Sea Scientific Drilling Program Well State 2-14." *Journal of Geophysical Research*, v. 93(B11), p. 13037-13045.
- Lachenbruch, A.H., J.H. Sass and S.P. Galanis, Jr., 1985. "Heat flow in Southernmost California and the Origin of the Salton Trough." *Journal of Geophysical Research*, 90(B8), p. 6709-6736.
- Yunker, L. W., P.W. Kasameyer, and J.D. Tewhey, 1982. "Geological, Geophysical, and Geothermal Characteristics of the Salton Sea Geothermal Field, California." *Journal of Volcanology and Geothermal Research*, v. 12, Issues 3-4, May 1982, p. 221-258.

¹ The term scalar gravity is used to mean what is commonly called gravity or microgravity, and to distinguish it from gravity gradiometry. Here, the term gravity methods encompasses both scalar gravity and gravity gradiometry.